

# $^1\text{H}$ and $^{13}\text{C}$ NMR characterization of pyridinium-type isoniazid–NAD adducts as possible inhibitors of InhA reductase of *Mycobacterium tuberculosis*

Sylvain Broussy,<sup>a</sup> Vania Bernardes-Génisson,<sup>a</sup> Yannick Coppel,<sup>a</sup> Annaïk Quémar,<sup>b</sup> Jean Bernadou<sup>\*a</sup> and Bernard Meunier<sup>a</sup>

<sup>a</sup> Laboratoire de Chimie de Coordination du CNRS, 205 route de Narbonne, 31077, Toulouse cedex 4, France. E-mail: bernadou@lcc-toulouse.fr; Fax: 33 (0)5 61 55 30 03; Tel: 33 (0)5 61 33 31 17

<sup>b</sup> Institut de Pharmacologie et de Biologie Structurale du CNRS, 205 route de Narbonne, 31077, Toulouse cedex 4, France

Received 24th November 2004, Accepted 23rd December 2004  
First published as an Advance Article on the web 21st January 2005

Oxidative activation of the antituberculous drug isoniazid (INH) in the presence of the NADH cofactor gives a pool of INH–NAD adducts proposed to be involved in the mechanism of action of this drug through inhibition of the reductase InhA. Among these adducts and besides dihydropyridine derivatives, two pyridinium-type isoniazid–NAD adducts were shown to be formed in solution and have been fully characterized by  $^1\text{H}/^{13}\text{C}$  NMR and MS. One of them results from the oxidation of dihydropyridine-type INH–NAD adducts. The spectral data strongly support its existence under two epimeric structures. These epimers arise from a cyclization process between the carboxamide group and the ketone function with the creation of a new chiral center at C-7. The second pyridinium-type adduct was formed in acidic solution by dehydration of the cyclized dihydropyridine-type INH–NAD adducts and also exists as a cyclized structure. Both of these pyridinium-type compounds were inactive as inhibitors of InhA activity and can be considered as deactivated species.

## Introduction

Tuberculosis is an infectious disease caused by *Mycobacterium tuberculosis* with a great impact in developing nations and in centers of urban decay. In the past two decades, there has been an important rise in the incidence of tuberculosis due, in part, to the widespread emergence of multidrug-resistant strains, which are strains resistant to at least the major first-line drugs used in combination chemotherapy: isoniazid and rifampicin. These recent aspects underscore the need for new drugs and stimulate the interest of researchers in elucidating the molecular mechanism of action of well-established antitubercular drugs as an aid in developing new therapeutics. Isoniazid (isonicotinic acid hydrazide, or INH) is a frontline antibiotic used since the 1950s in the treatment of tuberculosis.<sup>1,2</sup> INH exhibits little or no inhibitory activity against other mycobacteria and most prokaryotic pathogens. In fact, INH is a prodrug<sup>3–5</sup> and is activated by the mycobacterial catalase-peroxidase KatG to generate an active form, most likely the isonicotinoyl radical (Fig. 1). This active form binds covalently to the nicotinamide moiety of NADH<sup>6–10</sup> or NADPH,<sup>11</sup> coenzymes of the *trans*-2-enoyl-ACP reductase InhA (E.C.1.3.1.9)<sup>12,13</sup> and the  $\beta$ -ketoacyl-ACP reductase MabA, respectively.<sup>11</sup> Mycobacteria utilize the products of InhA and MabA catalysis to synthesize mycolic acids, long chain  $\alpha$ -branched fatty acids, which are major and specific components of the mycobacterial envelope.<sup>11,14,15</sup> Inhibi-

tion of this synthesis by INH–NAD adduct(s) has been proposed as being responsible for the lethal effect on bacterial cells. Indeed, an inactivation of InhA activity through a thermosensitive mutation leads to mycobacterial cell lysis.<sup>16</sup> Although a single isonicotinoyl–NAD adduct has been characterized within the active site of InhA by X-ray crystallography and this bound adduct was interpreted as the open dihydropyridine form **1** with a 4S configuration (Fig. 2),<sup>7</sup> the formation of several types of INH–cofactor adducts has been reported either by KatG-dependent activation,<sup>8,17</sup> by non-enzymatic  $\text{O}_2/\text{Mn}^{\text{II}}$  oxidation<sup>8,17,18</sup> or by using manganese(III) pyrophosphate (to mimic the mycobacterial KatG enzyme).<sup>9–11</sup> Initially, Wilming and Johnsson<sup>8</sup> described several species of INH–NAD adducts in dynamic equilibrium including 1,4-dihydropyridine- and pyridinium-type adducts. We recently proposed that six opened or cyclized INH–NAD adducts with a dihydropyridine structure were formed in solution (compounds **1–6**, Fig. 2), concomitantly with a low amount of oxidized derivatives.<sup>9–10</sup> These adducts have been shown, when tested as a purified pool, to be effective inhibitors of InhA.<sup>19</sup> The 1,4-dihydropyridine-type adducts were fully characterized.<sup>9–10</sup> In this work, we describe the preparation and the characterization of two INH–NAD pyridinium-type adducts formed in solution, including the adduct previously studied (but not fully characterized) by Wilming and Johnsson.<sup>8</sup> The potential interest of this category of molecules as effective inhibitors of InhA is discussed.

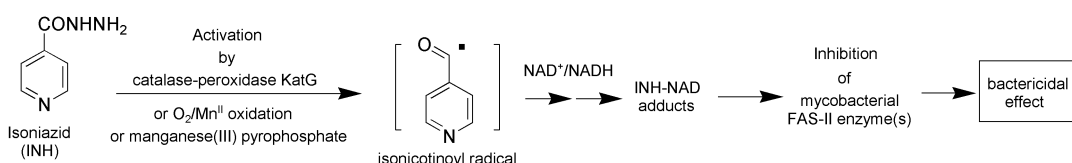
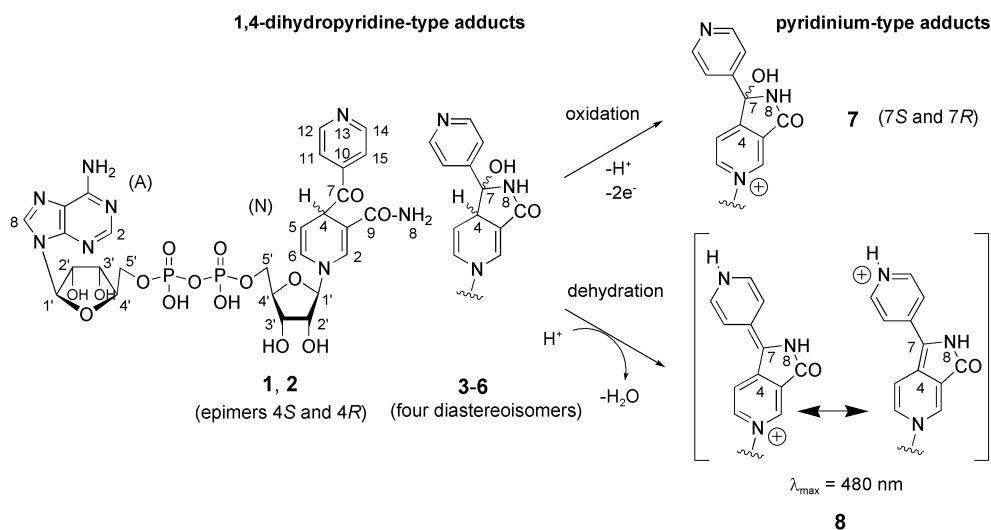


Fig. 1 Proposed mechanism of action of isoniazid. FAS-II is the fatty acid synthase system involved in biosynthesis of mycolic acids, that are specific components of the mycobacterial envelope.



**Fig. 2** Isoniazid–NAD 1,4-dihydropyridine-type and pyridinium-type adducts (**1** and **2** are the two epimers 4*R* and 4*S*; **3**, **4**, **5** and **6** are the four diastereoisomers 4*S*,7*R*, 4*R*,7*S*, 4*S*,7*S* and 4*R*,7*R*; **7** exists as two epimeric forms 7*R* and 7*S*).

## Results and discussion

### Preparation of the pyridinium-type INH–NAD adducts

Preparation of the pool of INH–NAD adducts obtained by biomimetic oxidation of INH in the presence of  $\text{NAD}^+$  has been previously described.<sup>9</sup> In the course of this operation we could observe secondary (minority) appearance of two types of rather stable adducts: one, compound **7** (existing as two epimers 7*R*/7*S*, see below), was formed under slow air oxidation and the other, compound **8**, was obtained by slow dehydration (Fig. 2). Although formation of compounds 7*R*/7*S* can be catalyzed by peroxidases as previously described<sup>8</sup> and can also be weakly accelerated by potassium ferricyanide, we found that uncatalyzed air oxidation was more suitable for HPLC purification of large amounts of this product. The dehydration reaction to give compound **8**, slow at neutral pH, could be very efficiently catalyzed by trifluoroacetic acid. As described in the experimental section, these two kinds of INH–NAD pyridinium-type adducts could be obtained with an acceptable purity of up to 95% determined by HPLC.

### Origin of the splitting of NMR signals in compounds 7 (*R/S*) and evidence of a stable cyclic hemiamidal structure

While various samples of adducts **7** (*R/S*) always gave a unique peak in HPLC analyses,<sup>8,9</sup> the NMR data of this collected peak showed split signals in a very reproducible manner (Fig. 3, to be compared with that published in ref. 8). The question of the corresponding structures was initially raised by Wilming and Johnsson<sup>8</sup> who suggested the existence of one pyridinium

open compound under two conformations, due to hindered rotation around the bond between the isonicotinoyl group and the C-4 atom of the nicotinamide ring, with different stacking interaction between the purine residue and the modified nicotinamide moiety in the two conformers.

Our careful  $^1\text{H}$  and  $^{13}\text{C}$  NMR analyses of the collected peak of adducts **7** (*R/S*) always showed two sets of signals in a ratio close to 1 : 1. This observation supports the coexistence of a pair of diastereoisomers rather than a pair of conformers as previously suggested.<sup>8</sup> The H1' (adenosine moiety) resonances (5.51 and 5.72 ppm) represent the most selective and convenient signal to distinguish the two compounds. The main NMR data are summarized in Fig. 4. In the two derivatives 7*R*/7*S*, the isonicotinoyl radical is bound at position 4 of the nicotinamide ring but, as for the previously elucidated structures of 1,4-dihydropyridine adducts **3–6**,<sup>10</sup> we could also imagine a cyclic hemiamidal structure with the creation of one additional chiral center at C-7. Then, the existence of two epimers could explain the splitting of the NMR signals, both in the vicinity of this chiral center and also at distance from it, through a probable change in the stacking interaction of adenine with the modified nicotinamide moiety. In fact, the key argument supporting such cyclized structures for compound **7** (*R/S*) is the determination of the trigonal (ketone structure) or tetrahedral (hemiamidal structure) character of C-7. Both adducts 7*R* and 7*S* exhibited a C-7 resonance at 86.6 ppm, characteristic of a tetrahedral carbon. The attribution of this resonance to C-7 was strongly confirmed by the  $^1\text{H}$ – $^{13}\text{C}$  HMBC spectrum of compounds **7** (*R/S*) exhibiting a well-defined  $^3J$  correlation between H-5 and C-7 (Fig. 5). Carbon-7 is the only tetrahedral carbon in a suitable position close to H-5 for such a correlation. Attribution of the signals at 8.00 and 7.97 ppm to H-5 (distinct signals for the two epimers) was firmly supported by  $^1\text{H}$ – $^1\text{H}$  and  $^1\text{H}$ – $^{13}\text{C}$  correlations between protons and carbons of the pyridinium ring. Consequently the two pyridinium adducts 7*R*/7*S* are epimers and have cyclized hemiamidal structures differing only by their stereochemistry at C-7. This observation is in agreement with our recent work in which we showed that a synthetic simplified pyridinium-type adduct is also found in the cyclized form.<sup>20</sup>

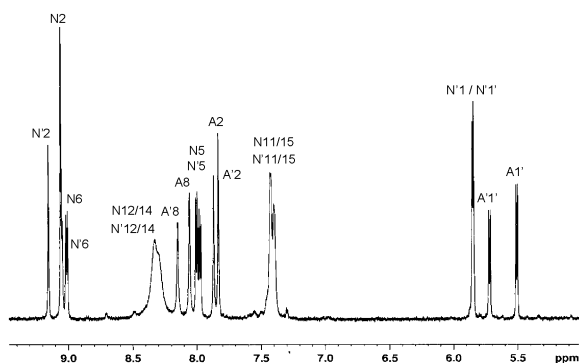


**Fig. 3** Section of the  $^1\text{H}$  NMR spectrum of compounds **7** (*R/S*) ( $\text{D}_2\text{O}$ , 500 MHz, 10 °C). The labeling of the peaks is as shown in Fig. 2; A and N refer to the adenine and nicotinamide moieties, respectively.

### Evidence of a stable cyclic structure for compound 8

Taking into account the data obtained from mass spectrometry, UV and NMR spectroscopy, we assigned to the compound **8** the structure shown in Fig. 2. The MS spectrum of this compound (ESI,  $m/z$  753) when compared with the MS spectra of the

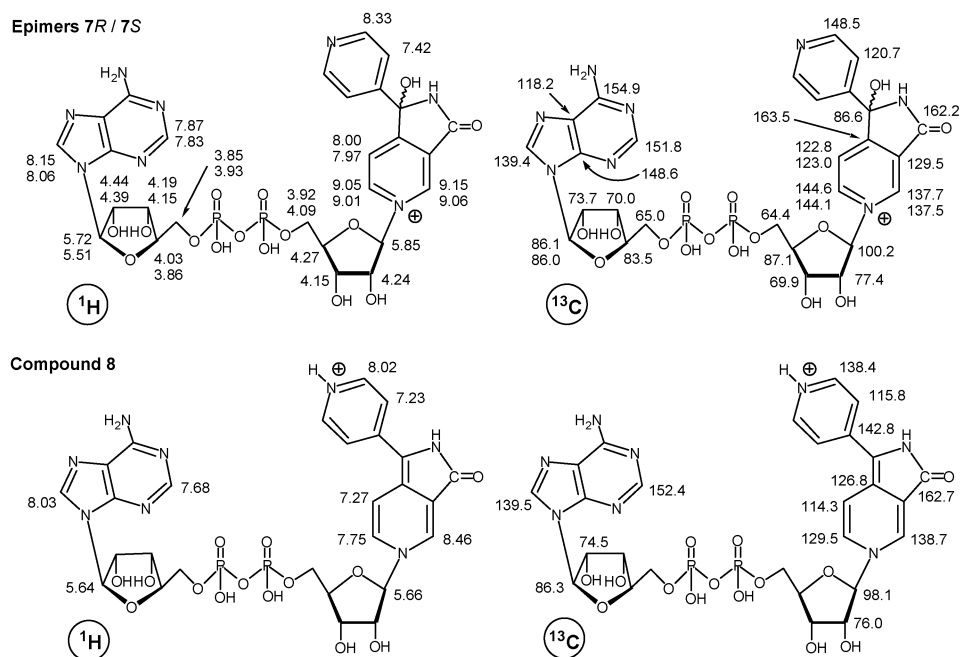


**Fig. 4**  $^1\text{H}$  (left) and  $^{13}\text{C}$  (right) NMR data for INH–NAD adducts **7R** and **7S** ( $\text{D}_2\text{O}$ , 500 MHz,  $10^\circ\text{C}$ ) and compound **8** ( $\text{D}_2\text{O}$ , 400 MHz,  $25^\circ\text{C}$ ). Distinct signals for each epimer of compound **7** are indicated when they were detected. Only signals which could be attributed on the basis of chemical shift,  $^1\text{H}$ – $^1\text{H}$  COSY,  $^1\text{H}$ – $^{13}\text{C}$  HMQC and HMBC experiments are depicted.

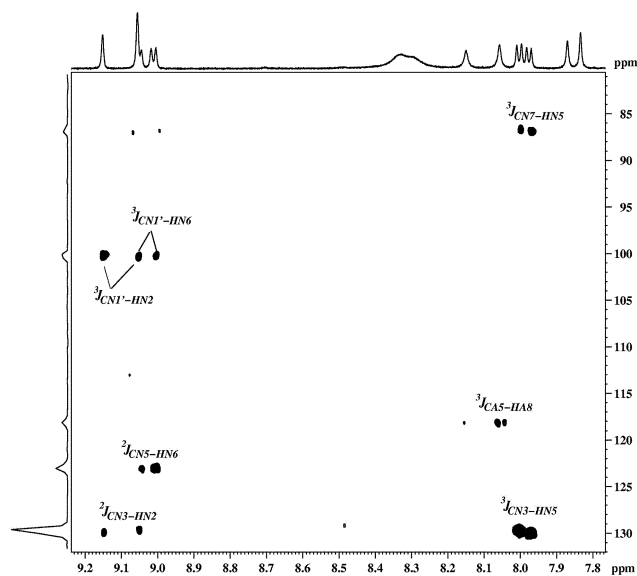


**Fig. 5** Two-dimensional  $^1\text{H}$ – $^{13}\text{C}$  HMQC long-range correlations for the mixture of epimers **7R** and **7S**.

dihydropyridine adducts (ESI,  $m/z$  771) indicates the loss of one water molecule. This highly conjugated compound **8** exists in two main mesomeric forms that explain the bathochromic effects observed in the UV-vis spectrum ( $\lambda_{\text{max}}$  480 nm, intense

red color). The  $^1\text{H}/^{13}\text{C}$  NMR spectra are also in agreement with the proposed structure. Although adduct **8** can be deprotonated in a mild alkaline medium ( $\text{p}K_{\text{a}}$  7.8) to give a yellow compound ( $\lambda_{\text{max}}$  400 nm), it mainly exists as the pyridinium form in neutral conditions.

#### InhA activity assays

Inhibition of InhA reductase activity by adducts **7R/7S** has been initially tested and the adducts found inactive by Wilming and Johnsson.<sup>8</sup> We assayed the inhibitory activity of compounds **7R/7S** and **8** in conditions previously described for the pool of adducts **1–6** (Table 1).<sup>19</sup> A weak inhibition could be detected at  $25\ \mu\text{M}$  (25% inhibition) for adduct **8** and the mixture of adducts **7R/7S** was found to be inactive at  $25\ \mu\text{M}$  while, in similar conditions, the dihydropyridine-type adducts **1–6** behave as strong inhibitors (at  $100\ \text{nM}$ , 78% inhibition was obtained). Taking these results into consideration, pyridinium adducts should be considered as inactive components of the pool of adducts previously assayed.<sup>19</sup>

#### Conclusion

Analyses by  $^1\text{H}/^{13}\text{C}$  NMR and MS allowed us to elucidate the structure of the pyridinium-type INH–NAD adducts **7R/7S**. It was shown that these adducts exist in solution as two epimeric structures resulting from a cyclization process that creates a new chiral center at C7. Another new derivative formed by

**Table 1** Inhibition of InhA activity by the isolated pool of dihydropyridine-type INH–NAD adducts **1–6** and by the pyridinium-type INH–NAD adducts **7** and **8**

Adduct	Adduct concentration	Remaining% of InhA activity	Ref.
Dihydropyridine-type	<b>1–6</b> (purified pool)	22	19
Pyridinium-type	<b>7R/7S</b>	100	8
	<b>7R/7S</b>	100	This work
	<b>8</b>	100	This work
	<b>8</b>	100	This work
	<b>8</b>	75	This work

<sup>a</sup> No published details on the experimental conditions used for this evaluation.

dehydration in acidic medium, compound **8**, has also been fully characterized and shown to be of pyridinium-type at physiological pH. These pyridinium-type compounds were shown to be devoid of InhA inhibitory activity. These data underline the role of the dihydropyridine adducts in the inhibition of InhA activity and so the dihydropyridine pharmacophore seems to be an important feature to take into account in the design of new specific InhA inhibitors for the development of potential antituberculosis agents. In a preliminary report, we have shown that the synthesis of a simplified pyridinium analogue of the INH–NAD adduct can be performed.<sup>20</sup> Further syntheses of dihydropyridine analogues are in progress and these derivatives will be evaluated as anti-mycobacterial compounds.

## Experimental

### Analytical methods

HPLC analyses were performed on a reverse-phase C18 column (nucleosil, 10  $\mu$ m, 250  $\times$  4.6 mm) using a linear gradient from 100% NH<sub>4</sub>OAc (70 mM) aqueous solution to 20% acetonitrile (flow rate: 1 mL min<sup>-1</sup>). Semi-preparative HPLC was performed on a reverse phase C18 column (nucleosil, 10  $\mu$ m, 250  $\times$  10 mm) using the same gradient. The columns were coupled to a diode array detector (Kontron) for the monitoring of UV-vis spectra detection of 1,4-dihydropyridine adducts **1–6** (at 260 nm and 330 nm) and pyridinium adducts **7R/7S** (at 260 nm) and **8** (260 and 480 nm).

LC–ESI–MS analyses. LC separations were performed under the conditions indicated above but with a quaternary pump. Only 4% of the flow eluted from the column was introduced into the electrospray source after automated mixing with a 1% HCOOH solution using a Harvard Apparatus syringe pump. The ESI–MS spectrometer was a Perkin-Elmer SCIEX API 365 and analyses were performed in the positive mode.

NMR spectra were recorded on a Bruker spectrometer at 400 and 500 MHz using D<sub>2</sub>O as solvent. Temp. 283 K.

InhA assays were performed on a Uvikon 923 spectrophotometer (Kontron) equipped with a circulating water bath for temperature control.

*M. tuberculosis* InhA was overexpressed in *E. coli* and purified as previously described.<sup>21</sup> Isoniazid and NAD<sup>+</sup> were obtained from Sigma-Aldrich. The substrate 2-*trans*-decenoyl-CoA was synthesized from 2-*trans*-deceanoic acid using the mixed anhydride method and purified according to the procedure described elsewhere.<sup>21</sup> The concentration of the substrate was determined on the basis of  $\epsilon_{260} = 16\,800\text{ M}^{-1}\text{ cm}^{-1}$ .<sup>21</sup>

### Preparation of the INH–NAD adducts 7R/7S

Preparation and purification of the pool of dihydropyridine INH–NAD adducts has been previously described.<sup>9,10</sup> In short, the reaction medium (15 mL final volume) contained INH (2 mM), NAD<sup>+</sup> (2 mM) and Mn<sup>III</sup>-pyrophosphate (4 mM) in 100 mM phosphate buffer pH 7.5 and was stirred at rt for 20 min. The pool of dihydropyridine adducts **1–6** was separated from other components of the reaction mixture using a Sep Pak<sup>®</sup> Vac 20 cc (5 g) cartridge. The reaction mixture was loaded into the cartridge and washed with 4 mM NH<sub>4</sub>OAc aqueous solution; only the pool of adducts was retained. Careful washing with water followed by elution with acetonitrile and concentration to dryness under vacuum afforded the pool of dihydropyridine adducts. At this step, the adducts **7R/7S** were only detected as traces (less than 5%). The pool of adducts was then dissolved in water (1 mL) and stirred at room temperature for approximately 2 days, until the HPLC profile showed nearly complete disappearance of the dihydropyridine adducts and appearance of the peak corresponding to the adducts **7R/7S** (retention time = 24 min), which was then purified by semi-

preparative HPLC. MS (ESI),  $m/z$  769. UV  $\lambda_{\text{max}}$  260 nm ( $\epsilon$  27 000 M<sup>-1</sup> cm<sup>-1</sup>).

### Preparation of the INH–NAD adduct 8

The pool of dihydropyridine adducts **1–6** was dissolved in dry DMSO (1 mL) and trifluoroacetic acid (10  $\mu$ mol, 20  $\mu$ L of a solution of 20  $\mu$ L TFA in 480  $\mu$ L DMSO) was added. A deep red colour appeared instantly. After 2 h, the reaction mixture was diluted with water and purified by semi-preparative HPLC (conditions described above). The product **8** eluted with a retention time of 29 min. MS (ESI),  $m/z$  753. UV  $\lambda_{\text{max}}$  480 nm (intense red color,  $\epsilon$  estimated 20 000 M<sup>-1</sup> cm<sup>-1</sup>).

### Inhibition of InhA

Inhibition of InhA activity by adducts **7R/7S** and **8** was tested as follows: 77 nM of InhA was preincubated for 5 min at 25 °C in the presence of 25  $\mu$ M of **7R/7S** or 1–25  $\mu$ M of **8** in 100 mM sodium phosphate buffer, pH 7.5, in a total volume of 800  $\mu$ L (concentrations calculated for a final volume of 1 mL). Reactions were initiated by adding 35  $\mu$ M decenoyl-CoA and 100  $\mu$ M NADH to a final volume of 1 mL. Enoyl reductase activity of InhA was assayed by monitoring the oxidation of NADH at 340 nm (25 °C) and initial velocities were determined. Results are expressed as percent of remaining InhA activity on the basis of control experiments, without potential inhibitor.

## References

- 1 K. Bartmann, H. Iwainki, H. H. Kleeberg, P. Mison, H. H. Offe, H. Otten, D. Tettenborn, L. Trnka, in *Antituberculosis drugs*, ed. K. Bartmann, Springer-Verlag, Berlin, 1988.
- 2 J. S. Blanchard, *Annu. Rev. Biochem.*, 1996, **65**, 215–239.
- 3 B. K. Sinha, *J. Biol. Chem.*, 1983, **258**, 796–801.
- 4 Y. Zhang, B. Heym, B. Allen, D. Young and S. Cole, *Nature*, 1992, **358**, 591–593.
- 5 K. Johnsson and P. G. Schultz, *J. Am. Chem. Soc.*, 1994, **116**, 7425–7426.
- 6 K. Johnsson, D. S. King and P. G. Schultz, *J. Am. Chem. Soc.*, 1995, **117**, 5009–5010.
- 7 D. A. Rozwarski, G. A. Grant, D. H. R. Barton, W. R. Jacobs Jr. and J. C. Sacchettini, *Science*, 1998, **279**, 98–102.
- 8 M. Wilming and K. Johnsson, *Angew. Chem., Int. Ed.*, 1999, **38**, 2588–2590.
- 9 M. Nguyen, C. Claparols, J. Bernadou and B. Meunier, *Chem-BioChem*, 2001, **2**, 877–883.
- 10 S. Broussy, Y. Coppel, M. Nguyen, J. Bernadou and B. Meunier, *Chem. Eur. J.*, 2003, **9**, 2034–2038.
- 11 S. Ducasse-Cabanot, M. Cohen-Gonsaud, H. Marrakchi, M. Nguyen, D. Zerbib, J. Bernadou, M. Daffé, G. Labesse and A. Quémard, *Antimicrob. Agents Chemother.*, 2004, **48**, 242–249.
- 12 A. Banerjee, E. Dubnau, A. Quémard, V. Balasubramanian, K. Sun Um, T. Wilson, D. Collins, G. de Lisle and W. R. Jacobs Jr., *Science*, 1994, **263**, 227–230.
- 13 A. Quémard, A. Dessen, M. Sugantino, W. R. Jacobs Jr., J. C. Sacchettini and J. S. Blanchard, *J. Am. Chem. Soc.*, 1996, **118**, 1561–1562.
- 14 K. Takayama, L. Wang and H. L. David, *Antimicrob. Agents Chemother.*, 1972, **2**, 29–35.
- 15 A. Quémard, C. Lacave and G. Lanéelle, *Antimicrob. Agents Chemother.*, 1991, **35**, 1035–1039.
- 16 C. Vilchère, H. R. Morbidoni, T. R. Weisbrod, H. Iwamoto, M. Kuo, J. C. Sacchettini and W. R. Jacobs Jr., *J. Bacteriol.*, 2000, **182**, 4059–4067.
- 17 B. Lei, C.-J. Wei and S.-C. Tu, *J. Biol. Chem.*, 2000, **275**, 2520–2526.
- 18 R. Rawat, A. Whitty and P. J. Tonge, *Proc. Natl. Acad. Sci. U. S. A.*, 2003, **100**, 13881–13886.
- 19 M. Nguyen, A. Quémard, S. Broussy, J. Bernadou and B. Meunier, *Antimicrob. Agents Chemother.*, 2002, **46**, 2137–2143.
- 20 S. Broussy, V. Bernardes-Génisson, H. Gornitzka, J. Bernadou and B. Meunier, *Org. Biomol. Chem.*, 2005, DOI: 10.1039/b415439h.
- 21 A. Quémard, J. C. Sacchettini, A. Dessen, C. Vilcheze, R. Bittman, W. R. Jacobs Jr. and J. S. Blanchard, *Biochemistry*, 1995, **34**, 8235–8241.